

Nonlinear modal analysis of nonconservative systems: Extension of the periodic motion concept

Malte Krack^{1,*}

Abstract

As the motions of nonconservative autonomous systems are typically not periodic, the definition of nonlinear modes as periodic motions cannot be applied in the classical sense. In this paper, it is proposed 'make the motions periodic' by introducing an additional damping term of appropriate sign and magnitude. It is shown that this generalized definition is particularly suited to reflect the periodic vibration behavior induced by harmonic external forcing or negative linear damping. In a large range, the energy dependence of modal frequency, damping ratio and stability is reproduced well. The limitation to isolated or weakly-damped modes is discussed.

Keywords: nonlinear normal modes, nonconservative systems, friction damping, Harmonic Balance, Shooting method, invariant manifold

1. Introduction

The concept of nonlinear modes is an attempt to extend the ideas of linear modal analysis to nonlinear systems. Nonlinear modal analysis is useful to characterize and quantify the energy dependence of the essential vibration behavior of nonlinear systems. This facilitates the understanding of phenomena like energy transfer, localization and modal interactions that may be caused by nonlinear effects. Moreover, nonlinear modes can be used for the purpose of model reduction. To this end, the problem is reduced to the typically two-

*Corresponding author

Email address: krack@ila.uni-stuttgart.de (Malte Krack)

dimensional subspace spanned by a specific nonlinear mode. This can greatly improve the computational efficiency of vibration predictions, which is crucial e. g. for design optimization and uncertainty analysis involving detailed models of nonlinear structures [1, 2]. For recent overviews on the general topic, the interested reader is referred to [3, 4].

Useful mathematical properties are lost when nonlinear effects become important. For this reason, the definition of nonlinear modes¹ is less straight forward. There are basically two different established definitions: (a) the periodic motion definition and (b) the invariant manifold definition.

According to definition (a), nonlinear modes are viewed as periodic motions of the autonomous nonlinear system [5, 6]. A family of periodic motions can be defined that are continuations with respect to the kinetic energy. These branches of periodic solutions of the equation of motion may or may not be connected to a corresponding linear mode at low energies. By using continuation and bifurcation analysis, interactions between different nonlinear modes can be resolved. The periodic motion definition directly associates properties of the flow to the modes such as its frequency and its asymptotic stability. Unfortunately, it does not apply to nonconservative systems, since their autonomous motions are typically only periodic at possible limit cycles, i. e. at specific energy values. Being inspired by the modes of damped linear systems, Laxalde and Thouverez [7] defined nonlinear modes as pseudo-periodic motions. They computed them by means of the generalized Fourier-Galerkin method. In contrast to the oscillatory term in the usual Fourier ansatz, they considered an additional decay term.

¹In literature, the term Nonlinear Normal Mode (NNM) is quite common. However, the term ‘normal’ may mislead to the wrong conclusion that nonlinear modes are orthogonal to each other. Apparently this term goes back to Rosenberg [5], who defined nonlinear modes as vibrations in *unison*, i. e. where all material points cross their equilibrium point and their extremum points simultaneously. For this type of vibration, the motions take place on so-called modal lines in the generalized displacement space which are normal to the surface of maximum potential energy [4]. However, this property is only valid for symmetric conservative systems. Hence the term ‘normal’ in this context is avoided throughout this article.

This approach is, however, strictly limited to trigonometric base functions, and the notion of mode stability has not been established yet.

According to definition (b), nonlinear modes are viewed as an invariant relationship between the coordinates of an autonomous system. This relationship defines a manifold in the system's phase space that includes the equilibrium point, where it is tangential to the hyper-plane spanning the locus of the corresponding linear mode [8, 9, 10]. In the simplest case without internal resonances, this manifold is two-dimensional. Hence, a point on the manifold can be parameterized uniquely by a suitable set of two coordinates. Only the geometry of the invariant manifold is governed by this definition. To assess the vibratory properties such as frequency and stability, the in-manifold flow can be analyzed in a second step. Conceptually, the invariant manifold definition is not limited to conservative systems. Compared to periodic motion based methods, two important difficulties are often reported in practice: the difficulty to find a suitable set of coordinates for a unique parametrization and the computational burden. The former difficulty often arises in conjunction with localization and modal interactions at higher energies. These phenomena can lead to a folding of the invariant manifold in certain coordinate systems, so that not every point on it can be described uniquely anymore, see e. g. [11, 12]. In terms of computational effort, it can generally be stated that periodic motion based procedures tend to be more efficient than invariant manifold based ones. For periodic motion based methods, only a single periodic orbit needs to be computed at the same time. In contrast, often the entire manifold, being the locus of infinitely many orbits, has to be determined simultaneously in the case of invariant manifold based methods. This results in a larger problem dimension and can produce considerable computational effort. To simplify the problem, the manifold can be divided into annular regions of finite size. But the unsteady character of the flow of nonconservative systems generally leads to a coupling of these regions, which requires special attention [12].

The purpose of this article is to extend the periodic motion definition to dissipative systems. The general concept is introduced in Section 2. Two computa-

tional implementations of the extended concept are outlined in Section 3. They are based on Shooting and Harmonic Balance, respectively. In Section 4, the capabilities and limitations of the approach are assessed for several numerical examples.

2. Extension of the periodic motion concept to dissipative systems

This section is divided into three subsections: First, the motivation and general idea for the extension of the periodic motion concept is presented. Then, the nonlinear modes are defined in such a way that they are capable of characterizing this dynamic regime in terms of eigenfrequency, modal damping ratio and vibrational deflection shape. Finally, analogies to the method of force appropriation are indicated.

2.1. Periodic vs. damped motion concept

Suppose the motions of an autonomous nonlinear system are described by a finite set of generalized coordinates \mathbf{u} and velocities $\dot{\mathbf{u}}$, governed by a set of second-order ordinary differential equations

$$\mathbf{M}\ddot{\mathbf{u}}(t) + \mathbf{f}(\mathbf{u}(t), \dot{\mathbf{u}}(t)) = \mathbf{0}. \quad (1)$$

Herein, \mathbf{M} is the mass matrix and \mathbf{f} are linear or nonlinear restoring as well as dissipative forces.

In the conservative case, the nonlinear modes represent periodic solutions to Eq. (1). Once the periodic motion is initiated, the autonomous system will retain this motion for all times. This motion can be initiated by according initial conditions. Also, this motion can be induced by harmonic external forcing at resonance, when an appropriate term is included into the autonomous Eq. (1). In other words, the frequency-energy characteristic of the nonlinear mode is identical to the backbone of the frequency response curves for varying excitation level. This is known as the ‘deformation-at-resonance’ property of nonlinear modes [13, 3].

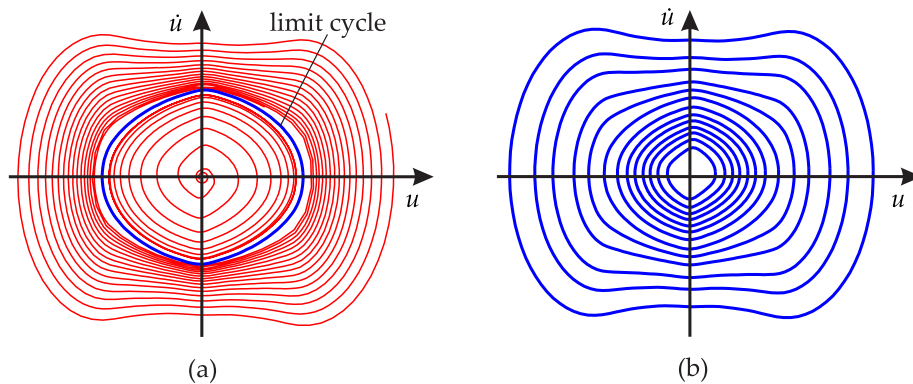


Figure 1: Visualization of different conceptions of nonlinear modes of nonconservative systems: (a) conventional damped motion concept, (b) periodic motion concept followed in this study

In the presence of nonconservative forces, an unsteady motion takes place instead until an attractor is reached, for instance a limit cycle or an equilibrium point. If the system is subjected to a harmonic external forcing at resonance, this behavior is changed and a periodic motion may persist instead. Depending on the excitation level, different kinetic energy levels can be reached. In the nonconservative case, the deformation-at-resonance property does not hold anymore, i.e. the backbone curve of the (steady-state) frequency response curves is not identical to the (instantaneous) frequency-energy characteristic of the autonomous system. In fact, this deviation is not due to nonlinearity, but also holds in the linear case: Consider the behavior of a single-degree-of-freedom oscillator with undamped eigenfrequency ω_0 and damping ratio D . While the backbone curve is a straight vertical line through the constant resonance frequency $\omega_{\text{res}} = \omega_0 \sqrt{1 - 2D^2}$, the frequency of the autonomous system is the damped eigenfrequency $\omega_d = \omega_0 \sqrt{1 - D^2}$.

Owing to this peculiarity of nonconservative systems, it is not ad hoc clear how to define the nonlinear modes. Essentially, there are two different opportunities:

- *damped motion concept*: nonlinear modes shall capture the strict autonomous behavior, i.e. unsteady motions in general, or
- *periodic motion concept*: nonlinear modes are still periodic motions, which

share, as much as possible, the properties of the underlying autonomous system

Both conceptions are illustrated in Fig. 1. The former concept is the classical one and was followed for instance in [12, 7]. In this study, the latter concept was followed. More specifically, periodic motions in the presence of (a) harmonic external forcing at resonance, and (b) self-excitation by negative modal damping represent the dynamic regime of interest. The aim is therefore to capture the vibration behavior in situations where a (permanent) *resonant excitation source* is present. The term ‘resonant’ refers to the fact that in both cases, the oscillation frequency equals one of the system’s (energy-dependent) eigenfrequencies. It is believed that this concept is more adjusted to persistent vibrations of nonconservative systems. Such vibrations are often of primary concern from a structural dynamic design point of view.

2.2. A new definition of nonlinear modes

The remaining question is now how to *make* the motions periodic. It is proposed to enforce periodicity by an additional damping term $\xi \mathbf{M}\dot{\mathbf{u}}$ that is just large enough to compensate the nonconservative forces,

$$\mathbf{M}\ddot{\mathbf{u}}(t) - \xi \mathbf{M}\dot{\mathbf{u}}(t) + \mathbf{f}(\mathbf{u}(t), \dot{\mathbf{u}}(t)) = \mathbf{0}, \quad 0 \leq t < T \quad \wedge \quad \mathbf{u}(t+T) = \mathbf{u}(t). \quad (2)$$

The extended definition of nonlinear modes is therefore as follows: *A nonlinear mode is as a family of periodic motions of an autonomous nonlinear system. If the system is nonconservative, these periodic motions are enforced by mass-proportional damping/self-excitation.*

The choice of a mass-proportional damping ensures consistency with linear modal analysis for the case of symmetric systems with modal damping. In this case, the nonlinear modes are orthogonal with respect to the mass matrix. Hence, the damping term does not affect the mode shape or the natural frequency ω_0 . The damping term is related to the modal damping by $2D\omega_0 = \xi$. In the nonlinear regime, however, the modes are no longer orthogonal, so that the additional damping term can induce artificial modal coupling. This makes

the approach intrusive. Owing to this possible source of inaccuracy, the valid dynamic regime will be restricted to *isolated modes* where strong modal interactions are absent. It should also be noted that, by definition, the concept is limited to periodic motions. Consequently the approach is not useful to capture quasi-periodic or even chaotic motions, which may also be encountered near resonance. In general, the autoparametric character induced by the additional term in Eq. (2) could trigger the emergence of non-periodic dynamic regimes [14, 15].

Akin to their linear counterpart, nonlinear modes are of course a mathematical concept, regardless whether the conventional or the proposed definition are used. Their usefulness resides in their ability to reflect the vibration behavior of nonlinear systems in the dynamic regime of interest. It is thus crucial to verify this physical significance of the modal characteristics. This is the objective of the numerical examples in Section 4.

2.3. Comparison to force appropriation

The interested reader might point out that instead of introducing an additional damping term, one might consider an external harmonic forcing that drives the system into resonance. An appropriate condition to ensure resonant behavior could be the phase lag criterion, which requires a 90° phase lag between excitation and response [16]. This procedure is known as force appropriation. Frequency or phase of the (generally multi-harmonic) external forcing generally have to be adjusted iteratively to meet the resonance criterion. This adjustment is not required for the method proposed in this study: The correct phase and frequency of the excitation is automatically ensured owing to the positive feedback of the velocity. This is an important advantage of the proposed method. Moreover, a damping measure ξ or D is directly obtained by the modal analysis, whereas such a measure is not obvious in the case of force appropriation.

3. Computational procedures

As the nonlinear modes were defined as periodic motions, standard methods for analyzing limit cycles can be applied to Eq. (2). Two different computational procedures are considered for the modal analysis in this study, which are described in the following. They were based respectively on the well-known Harmonic Balance and the Shooting method.

3.1. Harmonic Balance

For this method, the dynamic variables are expanded in a Fourier series truncated to harmonic order H with base frequency ω_0 , e. g.

$$\mathbf{u}(t) \approx a \Re \left\{ \sum_{n=0}^H \hat{\boldsymbol{\psi}}_n e^{in\omega_0 t} \right\}. \quad (3)$$

Herein, $\hat{\boldsymbol{\psi}}_n$ are the harmonics of the eigenvector and a is the modal amplitude. The $\hat{\boldsymbol{\psi}}_n$ may be complex-valued to allow for a phase lag between the coordinates. Due to this particular choice of base functions, the approximation is automatically periodic. The harmonic order H should be selected as large as necessary to ensure sufficient accuracy and as small as possible to avoid spurious computational effort. The substitution of Eq. (3) into the equations of motion (2) and subsequent Fourier-Galerkin projection gives rise to a set of nonlinear algebraic equations:

$$\begin{aligned} & \text{solve} && - (n^2 \omega_0^2 + \xi n \omega_0) \mathbf{M} \hat{\boldsymbol{\psi}}_n a + \\ & && \hat{\mathbf{f}}_n \left(\omega_0, a \hat{\boldsymbol{\psi}}_0, \dots, a \hat{\boldsymbol{\psi}}_H \right) = \mathbf{0} \quad \forall n = 0, \dots, H \\ & \text{subject to} && \hat{\boldsymbol{\psi}}_1^H \mathbf{M} \hat{\boldsymbol{\psi}}_1 = 1, \quad \Im \{ \hat{\boldsymbol{\psi}}_{1,k} \} = 0 \\ & \text{with respect to} && \{ \omega_0, \xi, \hat{\boldsymbol{\psi}}_0, \dots, \hat{\boldsymbol{\psi}}_H \} \text{ for } a \in [a_{\min}, a_{\max}]. \end{aligned} \quad (4)$$

Just as in the general linear case, two normalization conditions are imposed in order to overcome the otherwise under-determined problem. A mass normalization of the fundamental harmonic $\hat{\boldsymbol{\psi}}_1$ of the eigenvector was used in this study, which is also commonly applied in the linear case. Note that in Eq. (4),

H denotes the Hermitian transpose and should not be confused with the harmonic order H . Any eigensolution can be phase-shifted and will still satisfy Eq. (4). A phase normalization is therefore proposed, where the imaginary part $\Im\{\hat{\psi}_{1,k}\}$ of an arbitrary component of the fundamental harmonic eigenvector is set to zero. Applying the normalization to the fundamental harmonic $\hat{\psi}_1$ is reasonable since $\hat{\psi}_n = \mathbf{0}$ for $n \neq 1$ in the linear case. As an alternative to the mass normalization, a normalization with respect to the kinetic energy can be performed, which is also well-suited for the case of internal resonances [17]. It should be noticed that only super-harmonics have been considered in the formulation of Eq. (4) utilized in this study, although the approach can be extended in a straightforward manner to account for sub-harmonics.

Evaluation of the forces

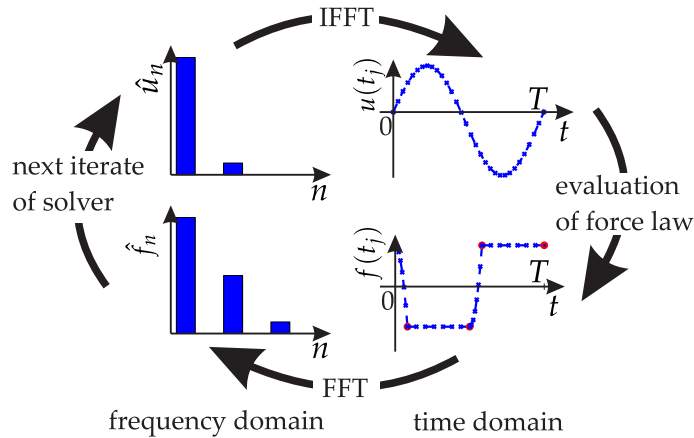


Figure 2: Alternating-frequency-time scheme

Since \mathbf{f} is generally nonlinear in \mathbf{u} and $\dot{\mathbf{u}}$, the harmonic components $\hat{\mathbf{f}}_n$ of the nonlinear forces also depend on the harmonics $a\hat{\psi}_1, \dots, a\hat{\psi}_H$ of the sought coordinates and on the eigenfrequency ω_0 . In general, this functional relationship cannot be expressed in closed form, and numerical procedures have to be utilized for computing $\hat{\mathbf{f}}_n$. The alternating-frequency-time scheme [18, 19] is a widely used technique in this context, and it is illustrated in Fig. 2. In each

iteration of the solver, the $\hat{\mathbf{f}}_n$ are evaluated to determine a new estimate for $\hat{\mathbf{u}}_n = a\hat{\psi}_n$. The inverse fast fourier transform (IFFT) is applied to determine the generalized coordinates $\mathbf{u}(t_j)$ and the velocities $\dot{\mathbf{u}}(t_j)$ at equally spaced time instants t_j . The force law is then directly evaluated in the time domain to obtain the force $\mathbf{f}(t_j)$. Finally, the harmonics $\hat{\mathbf{f}}_n$ are obtained by fast fourier transform (FFT). Mathematically, this procedure can be summarized as

$$\hat{\mathbf{f}} = \text{FFT} [\mathbf{f}(\text{IFFT}[\hat{\mathbf{u}}], \text{IFFT}[\omega_0 \nabla \hat{\mathbf{u}}])], \quad (5)$$

with $\mathbf{u} = \text{IFFT}[\hat{\mathbf{u}}]$ and $\dot{\mathbf{u}} = \text{IFFT}[\omega_0 \nabla \hat{\mathbf{u}}]$, where ∇ takes care of the differentiation in the frequency domain. This scheme makes it easy to take into account arbitrary nonlinear and even non-smooth forces.

Numerical solution

The eigenproblem in Eq. (4) comprises a number of $N_{\text{dim}} = N(2H + 1) + 2$ unknowns where N is the number of generalized coordinates. For the numerical solution, a variant of the Newton method was used. Specifically, the subroutine ‘fsolve’ was utilized, which is available in the Matlab software environment. This method requires the computation of the Jacobian, i. e. the matrix assembling the derivative of the residual vector with respect to the vector of unknowns. Throughout this study, the Jacobian was evaluated using analytical expressions. Typically the critical part is the derivation of the forces $\hat{\mathbf{f}}$. In the framework of the Alternating-frequency-time scheme, this can be achieved by utilizing the linearity of the FFT and the IFFT operator,

$$\frac{\partial \hat{\mathbf{f}}}{\partial x} = \text{FFT} \left[\frac{\partial \mathbf{f}(\mathbf{u}, \dot{\mathbf{u}})}{\partial \mathbf{u}} \cdot \text{IFFT} \left[\frac{\partial \hat{\mathbf{u}}}{\partial x} \right] + \frac{\partial \mathbf{f}(\mathbf{u}, \dot{\mathbf{u}})}{\partial \dot{\mathbf{u}}} \cdot \text{IFFT} \left[\frac{\partial \omega_0 \nabla \hat{\mathbf{u}}}{\partial x} \right] \right]. \quad (6)$$

Herein, the scalar variable x is one of the unknowns; i. e., it is either ω_0 , ξ , or the real or the imaginary part of a harmonic component of a generalized coordinate. The derivation of \mathbf{f} with respect to \mathbf{u} or $\dot{\mathbf{u}}$ is usually straight-forward. The interested reader is referred to [20, 21] more details and examples. After each evaluation of the residual function, thus, also its Jacobian is available, which is then provided to the nonlinear solver. This can greatly reduce the required

computational cost compared to the common finite difference approximations of the Jacobian. If the system features only localized nonlinearities, the nonlinear force vector is typically sparse. By exploiting this sparsity, the computational burden can be further reduced as demonstrated e. g. in [17].

For the iterative solution procedure, the considered linear mode was specified as initial guess at small amplitudes $a \approx 0$. Turning points with respect to the amplitude may be encountered, for instance in the presence of internal resonances. In order to overcome these turning points, a numerical path continuation was employed. The well-known predictor-corrector scheme with tangent predictor step and arc-length parametrization was used. The details of this scheme can be found e. g. in [22]. It should be noticed that more sophisticated bifurcation analysis techniques could be applied in a straight-forward manner, this was however considered beyond the scope of this study.

The different unknowns associated with Eq. (4) represent quite different physical quantities and may assume numerical values of different order of magnitude. This was found to have a crucial influence on the convergence behavior of the numerical solution procedure. A logarithmic scaling was used for the amplitude, as it typically undergoes comparatively large variations during the modal analysis. This is accomplished by treating $z := \log_{10} a$ rather than a as an unknown, and internally recovering $a = 10^z$, as needed. A linear scaling was applied to the remaining unknowns, so that they had approximately matching orders of magnitude.

Stability analysis

Owing to the periodic motion definition, the classical notion of asymptotic stability of limit cycles can be applied to the nonlinear modes. For the frequency domain, the Hill method can be employed [23, 24]. This basically involves the solution of a quadratic eigenvalue problem. The coefficient matrices of this problem only depend on quantities readily known from the solution of Eq. (4). Hence, the stability is typically analyzed a posteriori. Stability is determined by the real part of the Hill eigenvalues: If any of the eigenvalues has a positive

real part, the nonlinear mode is unstable at this point.

3.2. Shooting

For this method, periodic solutions of Eq. (2) are determined by solving the following boundary value problem:

$$\begin{aligned}
& \text{solve} && \begin{bmatrix} \mathbf{u}(T) \\ \mathbf{v}(T) \end{bmatrix} - \begin{bmatrix} \mathbf{u}_0 \\ \mathbf{v}_0 \end{bmatrix} = \mathbf{0} \\
& && \text{where } \mathbf{u}(T), \mathbf{v}(T) \text{ are obtained from:} \\
& && \begin{bmatrix} \dot{\mathbf{u}}(t) \\ \dot{\mathbf{v}}(t) \end{bmatrix} = \begin{bmatrix} \mathbf{v}(t) \\ -\mathbf{M}^{-1}\mathbf{f}(\mathbf{u}(t), \mathbf{v}(t)) + \xi\mathbf{v}(t) \end{bmatrix} \\
& && \text{with } \mathbf{u}(0) = \mathbf{u}_0, \mathbf{v}(0) = \mathbf{v}_0 \\
& \text{subject to} && u_{0,k} = q, \quad v_{0,k} = 0 \\
& \text{with respect to} && \{T, \xi, \mathbf{u}_0, \mathbf{v}_0\} \text{ for } q \in [q_{\min}, q_{\max}] \quad (7)
\end{aligned}$$

Herein, \mathbf{v} is the velocity $\mathbf{v} := \dot{\mathbf{u}}$. In addition to the initial values \mathbf{u}_0 and \mathbf{v}_0 , the period $T = \frac{2\pi}{\omega_0}$ and the damping coefficient ξ are unknown. For normalization, displacement $u_{0,k}$ and velocity $v_{0,k}$ of a particular coordinate at $t = 0$ are prescribed.

Numerical solution

Eq. (7) represents a set of nonlinear algebraic equations, which was solved like Eq. (4) using a variant of the Newton method in conjunction with a path continuation procedure. In each iteration of the solver, the states $\mathbf{u}(T)$ and $\mathbf{v}(T)$ at the end of the period T are determined by numerical time-step integration of Eq. (2) from the initial states $\mathbf{u}_0, \mathbf{v}_0$. The implicit average acceleration Newmark scheme was utilized in this study. It was also noted that other methods like the Runge-Kutta scheme work fine as well. If certain symmetries exist in the temporal evolution, the computational burden of the numerical integration can be reduced, as it is suggested e. g. in [25].

It should be remarked that the modal amplitudes a and q involved in the Harmonic Balance formulation (4) and the Shooting formulation (7), respectively,

cannot be directly compared. To make the results comparable, the Fourier transform was applied to the solution $\mathbf{u}(t)$ of Eq. (7). The modal mass $\hat{\mathbf{u}}_1^H \mathbf{M} \hat{\mathbf{u}}_1$ of the fundamental Fourier component $\hat{\mathbf{u}}_1$ equals the square a^2 of the modal amplitude in accordance with Eq. (4). Likewise, the harmonics $\hat{\boldsymbol{\psi}}_n$ of the eigenvector can be obtained. Moreover, it is useful to a posteriori derive other meaningful quantities from the frequency domain and the time domain results. In particular, the maximum value of a specific coordinate or the maximum kinetic energy were determined. The Jacobian of Eq. (7) was determined simultaneously to the actual integration process by integrating the derivative at each time step. This procedure is well-described e. g. in [22].

Stability analysis

The asymptotic stability of the periodic motions was analyzed in accordance with Floquet's theory. This involved computing the eigenvalues of the monodromy matrix. It should be noticed that this matrix is readily available from the computation of the Jacobian of Eq. (7).

4. Numerical examples

In order to validate the proposed methodology and to assess its computational performance, it was applied to various test cases. Three of these test cases are presented here, namely a van-der-Pol oscillator, a geometrically nonlinear two-degree-of-freedom system with viscous damping and a friction-damped rod.

4.1. Van-der-Pol oscillator

First, the van-der-Pol oscillator is considered with the following equation of motion

$$\ddot{u}(t) + \left(\frac{1}{10} u^2(t) - \alpha \right) \dot{u}(t) + u(t) = 0. \quad (8)$$

The purpose of this case study is to show the differences between periodic motion and damped motion concept of nonlinear modes, and to demonstrate the limitations of the proposed technique in the presence of strong damping.

Modal characteristics

A common approach to approximate the dynamic behavior of the van-der-Pol oscillator is the so-called ‘harmonic linearization’ technique. To this end, the displacement and the velocity are approximated in the form $u(t) \approx a \cos \omega_0 t$ and $\dot{u}(t) \approx -\omega_0 a \sin \omega_0 t$, respectively. Inserting these expressions into Eq. (8) and truncating the resulting expressions to their fundamental harmonic component gives rise to amplitude-dependent equivalent stiffness and damping values, see e.g. [26]. Just like in the case of a linear oscillator, approximate undamped eigenfrequency and damping ratio can thus be determined. For this case, this procedure yields

$$\omega_0(a) \approx 1, \quad D(a) \approx \frac{a^2}{80} - \frac{\alpha}{2}. \quad (9)$$

It should be noted that throughout this article, D denotes the modal damping ratio and is related to ξ , as defined in Eq. (2), by $2D\omega_0 = \xi$.

It can be ascertained from Eq. (4) that the proposed Harmonic Balance implementation of the periodic motion concept degenerates to the harmonic linearization approach for the special case of a single-degree-of-freedom oscillator if only the fundamental harmonic component $n = 1$ is considered. It was verified that the results for both approaches are identical in the case of $H = 1$, so that only one result will be shown in the following.

Furthermore, the governing equations (4) based on the Harmonic Balance procedure are similar to the ones derived with the generalized Fourier-Galerkin method in [7]. The methods even produce the same results in the special case when $D = 0$, i. e. at limit cycles of the original autonomous system. This mathematical similarity is remarkable since the authors of [7] followed a damped motion concept of the nonlinear modes, in contrast to the periodic motion concept pursued in the present study. Their method was also applied to analyze the van-der-Pol oscillator for comparison.

The modal characteristics of the van-der-Pol oscillator for a zero viscous damping coefficient of $\alpha = 0$ are depicted in Fig. 3. The results were computed by solving Eq. (4) for the case of harmonic orders $H = 1$ and $H = 13$. They were

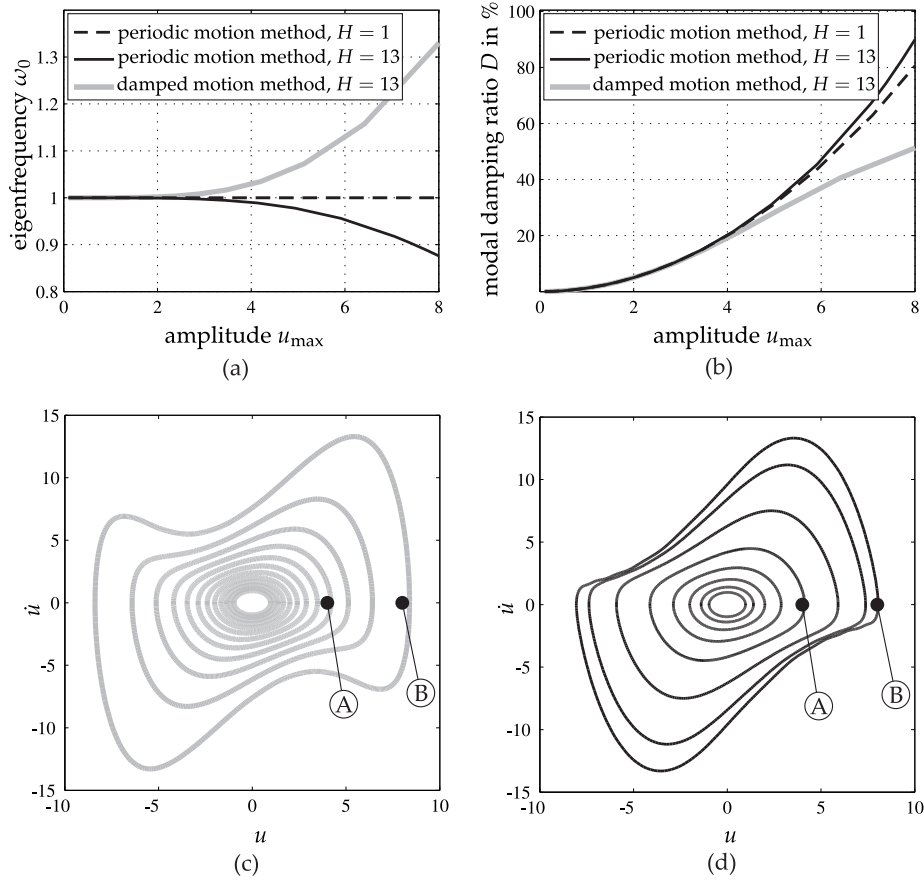


Figure 3: Modal characteristics of the van-der-Pol oscillator for $\alpha = 0$: (a) eigenfrequency, (b) damping ratio, (c) phase curves according to damped motion concept with $H = 13$, (d) phase curves according to periodic motion concept with $H = 13$

also computed by the damped motion method, i. e. the generalized Fourier-Galerkin method which is based on the damped motion concept [7]. The amplitude u_{\max} is the maximum time-domain displacement (considering all harmonics). Apparently, the results differ for large amplitudes, i. e. when the nonlinear effects become important. The frequency-amplitude characteristics exhibit strong differences in the regime of larger damping, e. g. $D > 20\%$. The same is true for the phase curves depicted in Fig. 3c-d. It should be noticed that these results only indicate that damped and periodic motion concept lead

to significantly different results. However, it is not a priori clear which modal characteristics are more ‘accurate’ in a suitable sense. This aspect is addressed next. In general, the damped motion concept is specifically designed to reflect the strictly autonomous (decaying or growing) oscillations of the system, while the periodic motion concept was designed to reflect the (almost) periodic response in the presence of forced or self-excitation. Two different cases were considered to investigate the ability of the modal characteristics to reflect the dynamic behavior of the nonlinear system: free decay with $\alpha = 0$, and limit cycles for varying $\alpha > 0$.

Free decay

First, the free decay is considered. To approximate the dynamic behavior using the computed modal characteristics, the method developed in [1] was applied. To this end, the temporal evolution of the amplitude a is governed by the following differential equation,

$$\dot{a}(t) = -D(a(t))\omega_0(a(t))a. \quad (10)$$

Eq. (10) was solved using, one after the other, the modal characteristics $D(a)$, $\omega_0(a)$ obtained by the periodic motion and the damped motion method. The results are depicted in Fig. 4 and compared to the reference results obtained from direct time step integration of Eq. (8). The reference envelope (dashed line) is defined as $\pm(u + \dot{u})$.

The most significant differences are expected in the regime of considerable nonlinear damping, because here $\omega_0(a)$ and $D(a)$ deviate from each other, see Fig. 3. However, in this regime the envelopes are almost indistinguishable. For lower initial energies (point A), the agreement with the reference is reasonably good. In contrast, the accuracy is poor for larger initial energies (point B), regardless of the input modal characteristics $\omega_0(a)$ and $D(a)$. The reason for this deviation is that Eq. (10) governs only the approximate slow dynamics nonlinear mode, since an averaging formalism was applied for fast time scale related to the oscillation with frequency ω_0 [1].

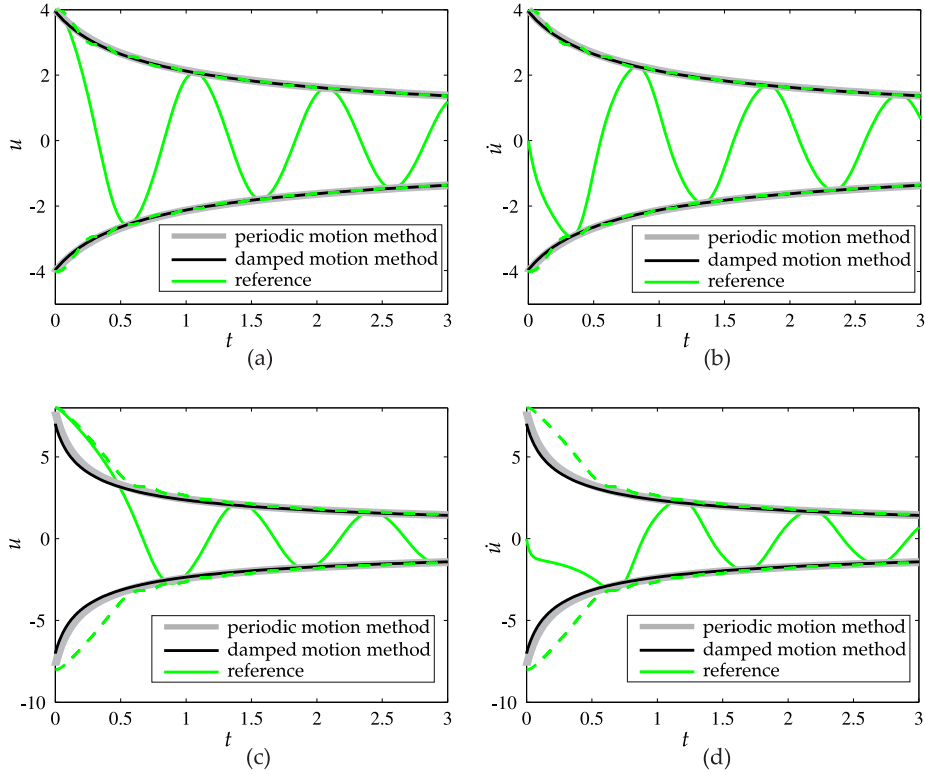


Figure 4: Time history of the free decay of the van-der-Pol oscillator: (a) displacement and (b) velocity for the point A, (c) displacement and (d) velocity for the point B indicated in Fig. 3c-d

Limit cycles for varying linear damping

Next, limit cycles for varying self-excitation intensity, i. e. varying α were investigated. The steady-state reference results were obtained by time integration of Eq. (8). The nonlinear mode based approximation was determined by solving the following algebraic equation with respect to the modal amplitude a [17]:

$$0 = 2D(a)\omega_0(a) - \alpha. \quad (11)$$

Herein, $D(a), \omega_0(a)$ are the modal characteristics computed for $\alpha = 0$. It is thus assumed that nonlinear and linear damping can be ‘superimposed’ as it is done in Eq. (11). Eq. (11) was solved using, one after the other, the modal charac-

teristics obtained from the respective periodic motion based and the damped motion based method.

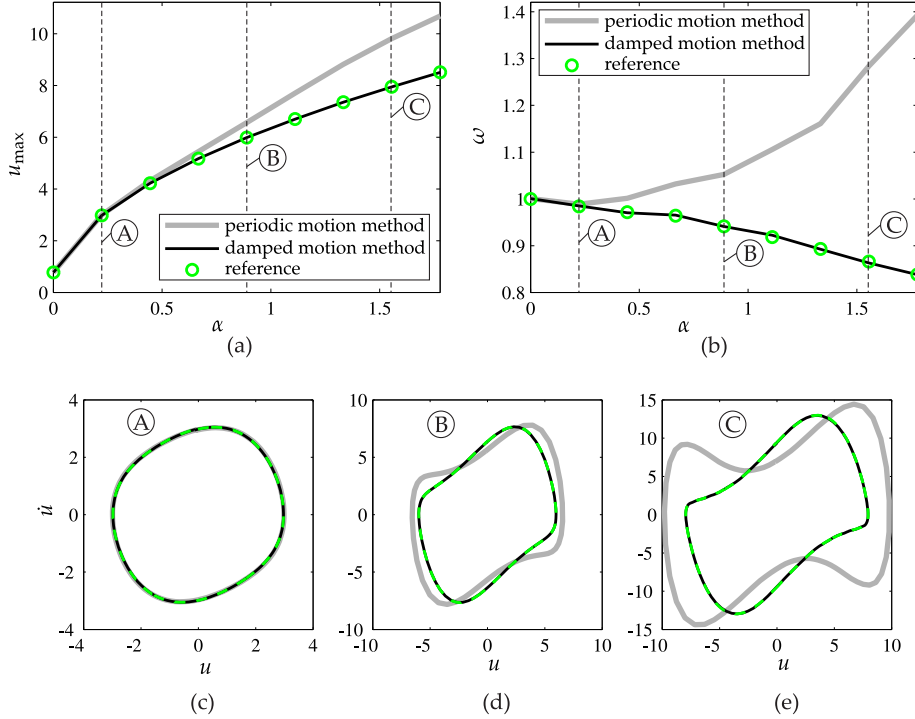


Figure 5: Limit cycle oscillations of the van-der-Pol oscillator for varying linear damping α : (a) amplitude, (b) frequency, (c)-(e) phase curves for $\alpha = 4/9, 8/9, 15/9$ respectively

The limit cycle amplitude u_{\max} , frequency ω and phase curve are illustrated in Fig. 5 for a varying damping coefficient α . The results based on the periodic motion concept agree perfectly with the reference results. This is expected since the artificial damping term $\xi \mathbf{M} \dot{\mathbf{u}}$ introduced for the modal analysis in Eq. (2) has the same effect as the damping term $\alpha \dot{u}$ in Eq. (8). In contrast, the results based on the damped motion concept exhibit a poor agreement for $\alpha \gg 0$. The reason for this deviation is that damped motions for $\alpha = 0$ were assumed for the modal analysis rather than limit cycles. In fact, even the qualitative dependence of the limit cycle frequency on α is not correctly predicted.

In conclusion, the proposed approach performs better than the conventional one in situations where one is actually interested in the steady flow of non-conservative systems with a permanent excitation source. On the other hand, damped motions are - by design - not very well reproduced by the proposed method.

4.2. Two-springs system with viscous damping

The system depicted in Fig. 6 is now considered. It consists of a single point mass attached to the ground via two linear springs. The system can undergo large deflections resulting in a geometric nonlinearity. This well-known problem was already investigated e. g. in [27, 28, 11, 12]. The motions of the system are governed by the following set of ordinary differential equations:

$$\ddot{u}_1 + 2\zeta_1\omega_1\dot{u}_1 + \omega_1^2 u_1 + \frac{\omega_1^2}{2}(3u_1^2 + u_2^2) + \omega_2^2 u_1 u_2 + \frac{\omega_1^2 + \omega_2^2}{2} u_1 (u_1^2 + u_2^2) = 0 \quad (12)$$

$$\ddot{u}_2 + 2\zeta_2\omega_2\dot{u}_2 + \omega_2^2 u_2 + \frac{\omega_2^2}{2}(3u_2^2 + u_1^2) + \omega_1^2 u_1 u_2 + \frac{\omega_1^2 + \omega_2^2}{2} u_2 (u_1^2 + u_2^2) = 0. \quad (13)$$

If the nonlinear terms are neglected, the system features two modes, one where the point mass oscillates vertically with the natural frequency ω_1 , and one where it oscillates horizontally with the natural frequency ω_2 . For sufficiently small amplitudes, the motions in these two orthogonal directions can be regarded as decoupled. As the amplitudes grow, the geometric nonlinearity causes a coupling between these motions [28]. As in [28], linear viscous damping terms are considered. An interesting feature of the system is that for certain parameter ranges, damping may change the nonlinear system behavior from a hardening to a softening behavior [28]; i. e., the qualitative dynamic behavior is non-trivial and cannot be explained by the underlying conservative system alone. This makes the system an ideal test case for the validation of the proposed methodology.

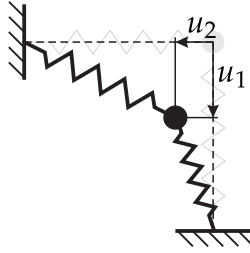


Figure 6: Model of a geometrically nonlinear oscillator with two linear springs

Modal characteristics

The modal characteristics of the first nonlinear mode were computed using the Harmonic Balance and the Shooting method, i. e. by solving Eq. (4) and Eq. (7), respectively. The results are depicted in Fig. 7 for the parameters listed below the figure. The Harmonic Balance results are labeled with a ‘HB’. The frequency-energy dependence and the geometry of the invariant manifold generally resemble previously reported results obtained by normal form theory [28] or a Galerkin-based approach for computing the invariant manifold [12]. In particular, the eigenfrequency first increases slightly with the kinetic energy and then decreases again. It should be remarked that in absence of damping, only a hardening effect would be observed. Hence, the damping has an essential influence on the qualitative vibration behavior. It should be noticed that the modal damping ratio is comparatively small, see Fig. 7b. This seems counter-intuitive owing to the crucial influence of the damping on the dynamic behavior. Apparently, the distribution of damping plays a more important role than its extent.

The use of Harmonic Balance also sheds some light into the underlying dynamics of the system: For larger energies, an important nonlinear interaction occurs between the first and the second mode. In the linear case these modes are close to a 2 : 1 internal resonance, $2\omega_1 = 2 \cdot 1.13 \approx 2 = \omega_2$. As a consequence, the second coordinate participates significantly in the second harmonic component of the motion. Hence, the second and higher harmonics play an important role in the qualitative evolution of the modal properties, as it can be seen in Fig. 7a-

b. Moreover, this can be ascertained from the invariant manifolds depicted in Fig. 7c-d: During one cycle of oscillation, the coordinate u_2 assumes two maxima and two minima, while the coordinate u_1 only assumes one maximum and one minimum.

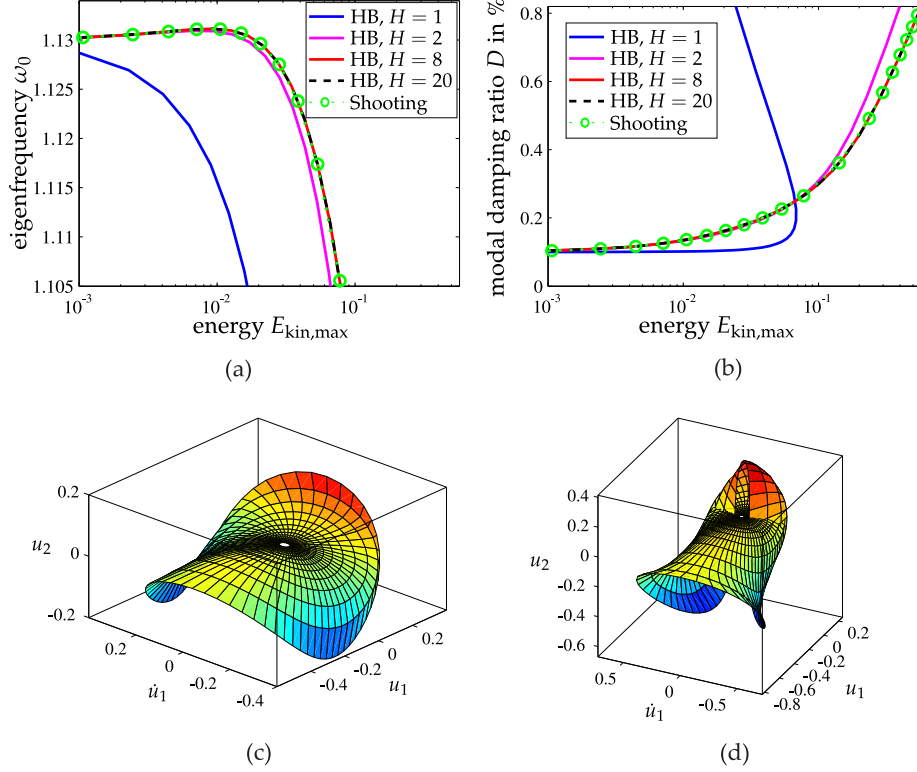


Figure 7: Modal characteristics of the first mode of the two-springs system: (a) eigenfrequency, (b) damping ratio, (c) and (d) invariant manifold prior to and beyond the fold, respectively; $\omega_1 = 1.13, \omega_2 = 2, \zeta_1 = 10^{-3}, \zeta_2 = 5 \cdot 10^{-3}$

As expected, the results obtained by Harmonic Balance are indistinguishable from the ones obtained by Shooting for a sufficiently large number of time steps per period and a sufficiently large number of harmonics. Several harmonics need to be retained to achieve asymptotic convergence of the modal characteristics. If only a single harmonic is considered ($H = 1$), only a softening behavior is predicted. The folding of the invariant manifold, as indicated in Fig. 7d, may

lead to parametrization problems if an invariant manifold based approach for the modal analysis is pursued. In contrast, the folding does not lead to any special attention when using the proposed procedure.

Forced response

The steady-state forced response of the two-springs system was also investigated. A harmonic excitation was applied to the point mass in both coordinate directions, with the same magnitude and equal phase. Hence, additional forcing terms have to be considered on the right hand side of Eq. (13). The Shooting method was applied to the resulting equations. The frequency range around ω_1 was considered. A predictor-corrector path continuation scheme was applied to overcome the turning points.

The frequency response curves of coordinate u_1 are depicted in Fig. 8a-b for different excitation levels. The maxima of the frequency response curves match well the backbone curve, which represents the frequency-amplitude characteristic of the nonlinear mode. This is true for all depicted excitation levels, in spite of the fact that the resonant response loses its asymptotic stability for large excitation levels, as indicated in Fig. 8b, and in spite of the folding of the invariant manifold at these energy levels, cf. Fig. 7d. In the presence of damping, the frequency at the maximum forced response does of course not exactly coincide with the undamped eigenfrequency. Note that this is also true in the linear case. However, as it can be ascertained from Fig. 7b, the modal damping ratio is comparatively small, so that this difference cannot be seen in Fig. 8a-b. From the high accuracy of the frequency-amplitude characteristic, it can be concluded that the introduction of the artificial damping term in Eq. (2) does not diminish the integrity of the proposed approach for this test case.

The asymptotic stability of the periodic motions was also investigated by means of Floquet's theory. To this end, the eigenvalues of the associated monodromy matrix were analyzed. It should be noticed that this is a comparatively inexpensive post-processing step in conjunction with the Shooting method. As expected, the overhanging part of the frequency response curves between the

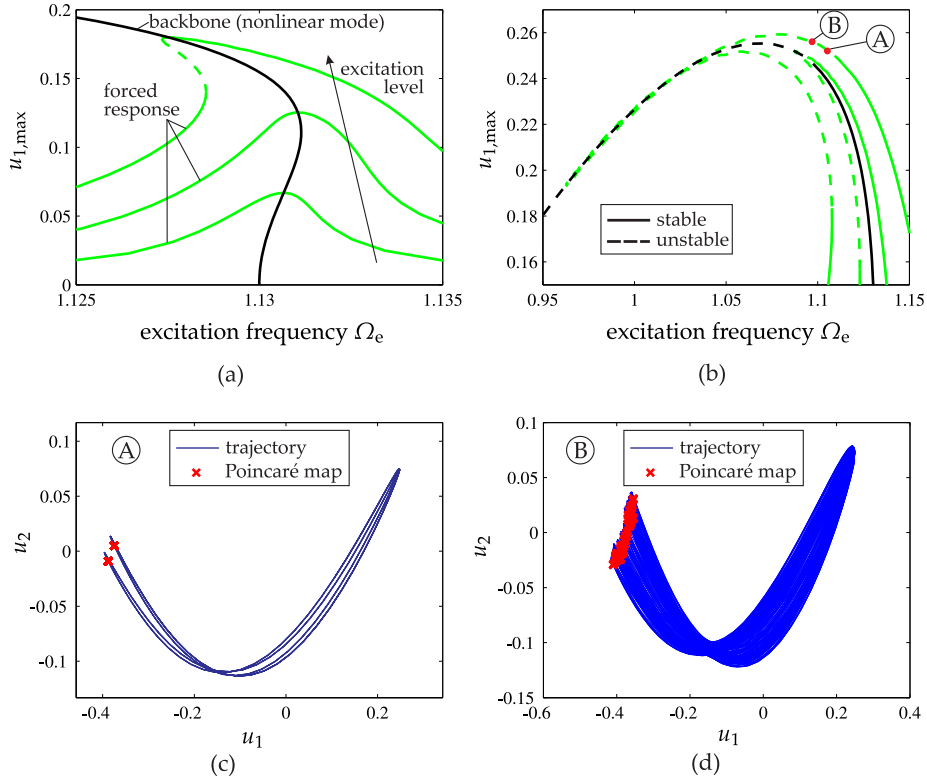


Figure 8: Forced response of the two-springs system: (a)-(b) amplitude-frequency curves and backbone for lower and higher excitation levels, (c)-(d) stable phase projections in the displacement space for two cases where the one-periodic response is unstable

two turning points is unstable. At the bifurcation points, a Floquet eigenvalue exits the unit circle in the complex plane at $+1$ on the real axis. This indicates a saddle node bifurcation. Starting from a point on the unstable branch, a transient motion would be initiated until a steady-state vibration on one of the stable branches is reached. Since the maximum of the frequency response curve is not on the overhanging branch, this type of instability is not present in the backbone curve.

Beyond a certain excitation level, a part of the frequency response around the resonance becomes unstable as well. In this case, a Floquet eigenvalue exits the unit circle in the complex plane at -1 on the real axis at the bifurcation

points. This indicates a period doubling bifurcation. To the best of the author’s knowledge, this type of bifurcation was not reported so far for the considered system [28, 12]. To confirm this behavior, the points A and B in Fig. 8b are considered, which are on the unstable section of one of the frequency response curves. Starting from the corresponding initial state $\mathbf{u}_0, \mathbf{v}_0$, the transient dynamic behavior was determined by means of direct time-step integration. After a certain number of transient periods, the motion was found to be steady. The motion starting from point A reaches a periodic orbit with frequency $2\Omega_e$, see Fig. 8c. This is in accordance with the results of the stability analysis. In contrast, the motion starting from point B does not reach a periodic orbit but approaches a non-periodic, possibly quasi-periodic attractor, see Fig. 8d. Apparently, bifurcations other than the considered flip bifurcation take place in this regime.

Remarkably, the point ($\Omega_e \approx 1.1$, $u_{1,\max} \approx 0.24$) and the type of stability loss of the forced response are in good agreement with the stability analysis of the nonlinear mode. Apparently, the nonlinear modes defined in Eq. (2) capture not only the frequency-energy dependence but also the asymptotic stability of 1 : 1 external resonances.

4.3. Friction-damped rod

Friction damping is a well-known means of accomplishing vibration reduction [29, 30]. The damping effect is achieved by the dissipative character of dry friction occurring in mechanical joints. Friction damping is particularly suited for the passive vibration reduction of lightly damped structures. Various applications can be found in the field of aerospace structures, combustion engines or turbomachinery blades. For the design of a friction-damped system, different performance measures are of particular interest: In externally forced scenarios, the resonance frequency shift is crucial for the detection and avoidance of possible resonances [31]. In self-excited scenarios, the effective damping ratio is often assessed [32, 33]. The proposed method is well-suited to determine these performance measures directly and thus represents an apt alternative to the crude

forced response simulations widely-used in this context.

A simple model of a slender friction-damped rod illustrated in Fig. 9 is considered. The rod of length ℓ is clamped at one end and it is connected to an elastic Coulomb dry friction element at its other end. Only small longitudinal vibrations of the rod were assumed, and the material was considered as homogeneous and linear elastic, with a Young's modulus E and a density ρ . The equations of motion of the continuous system can be summarized as follows:

$$\text{local equilibrium} \quad \rho \frac{\partial^2 u}{\partial t^2}(x, t) - E \frac{\partial^2 u}{\partial x^2}(x, t) = 0, \quad 0 < x < \ell, \quad (14)$$

$$\text{fixed boundary} \quad u(0, t) = 0, \quad (15)$$

$$\text{friction contact} \quad EA \frac{\partial u}{\partial x}(\ell, t) = -f_R [u(\ell, t)], \quad (16)$$

$$\text{elastic Coulomb law} \quad df_R = \begin{cases} k_t du & \text{if } |f_R + k_t du| < \mu N \\ 0 & \text{otherwise} \end{cases}. \quad (17)$$

Note that the elastic Coulomb law for the friction force f_R is written in differential form, where k_t denotes the contact stiffness and μN is the limit friction force.

The structural dynamic behavior of the rod was approximated using a finite element procedure. To this end, 20 rod elements of equal length $\ell_e = \ell/20$ were defined, each having the following consistent element mass and stiffness matrices [34]:

$$\mathbf{M}_e = \frac{\rho A \ell_e}{6} \begin{bmatrix} 2 & 1 \\ 1 & 2 \end{bmatrix}, \quad \mathbf{K}_e = \frac{EA}{\ell_e} \begin{bmatrix} 1 & -1 \\ -1 & 1 \end{bmatrix}. \quad (18)$$

Herein, A is the cross section area.

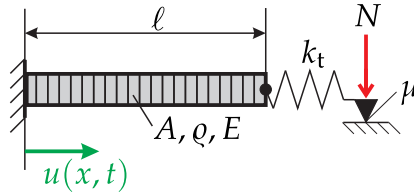


Figure 9: Model definition of the friction-damped rod undergoing longitudinal vibrations

Modal characteristics

The first nonlinear mode was analyzed using the Harmonic Balance and the Shooting method, i. e. by solving Eq. (4) and Eq. (7), respectively. The energy dependence of the modal frequency, damping ratio and the invariant manifold is depicted in Fig. 10. Throughout the figures in this subsection, some quantities are normalized which is indicated with an asterisk (*). Frequencies were normalized by the eigenfrequency in the linear case with sticking contact.

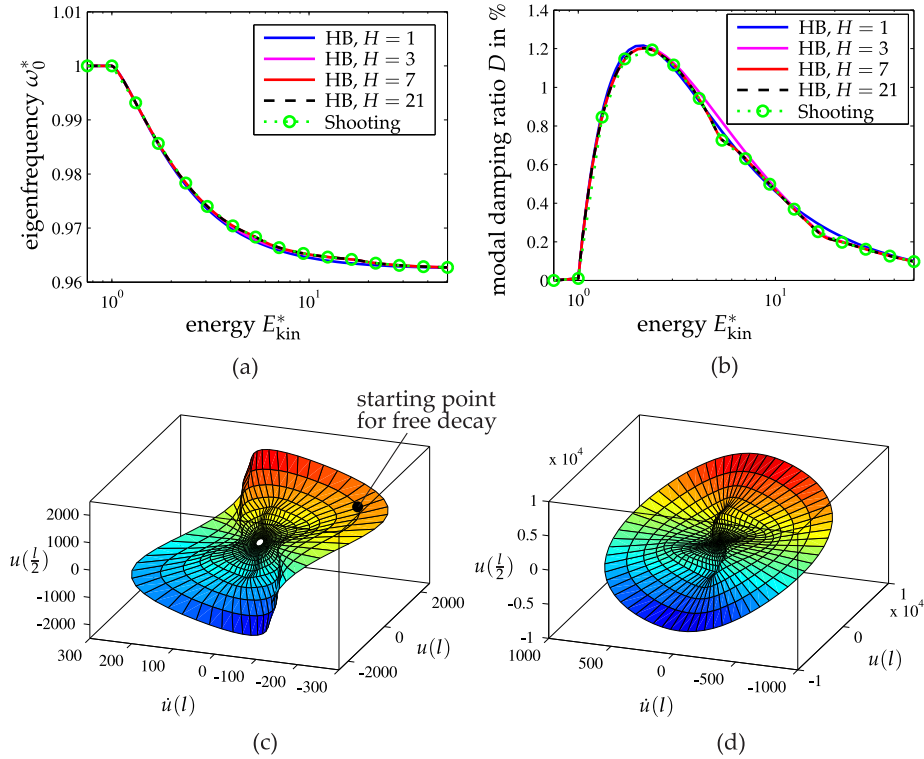


Figure 10: Modal characteristics of the first longitudinal mode of the friction-damped rod: (a) eigenfrequency, (b) damping ratio, (c)-(d) invariant manifold for different energy ranges; $\ell = 20, A = 1, \rho = 1, E = 1, k_t = 0.005, \mu N = 1$

For low kinetic energies, the friction element is only sticking, which results in a constant eigenfrequency and zero damping. Beyond this linear regime, the friction contact undergoes slipping in addition to sticking. The kinetic energy

E_{kin} was normalized by its value at the end of the linear energy regime, i. e. when slipping occurs for the first time instead of only sticking. The slipping phases cause a softening and a damping effect. For large energies, sliding friction dominates, and the modal frequency approaches the eigenfrequency of the linear rod without friction contact. The dissipated energy grows linearly with the displacement amplitude. For comparison, it would grow quadratically for a linear viscous damper, for which D would be constant. Hence, the effective damping ratio D of the friction-damped system tends towards zero. The modal characteristics qualitatively resemble the results previously reported by other researchers, see e. g. [35, 36, 7].

In Fig. 10c-d, the two-dimensional invariant manifold is depicted for different energy levels in a three-dimensional subspace of the 40-dimensional phase space. The closed curves correspond to the computed periodic motions. Apparently, the orbits deviate from ellipses, which indicates higher harmonic content of the periodic motions. Moreover, the orbits do not lie in a plane anymore, which indicates that the mode shape also depends on the kinetic energy. This behavior is certainly influenced by the non-smooth character of the dry friction forces. The results obtained from the Shooting and the Harmonic Balance method are in good quantitative agreement. It should be noticed that frequency-energy and damping-energy characteristic do not significantly depend on the harmonic order H , even though the multi-harmonic character of the periodic motions can be easily ascertained from the invariant manifold.

Free decay

The free decay of the first nonlinear mode was investigated next. The starting point is indicated in Fig. 10c. The temporal evolution of the modal amplitude was approximated by numerical integration of Eq. (10). For reference, the time history of the coordinates was determined by numerical integration of the full set of equations of motion (1).

The results for the evolution of the rod's tip displacement $u(\ell)$ are shown in Fig. 11. In addition to the envelope, the synthesized temporal evolution of $u(\ell)$

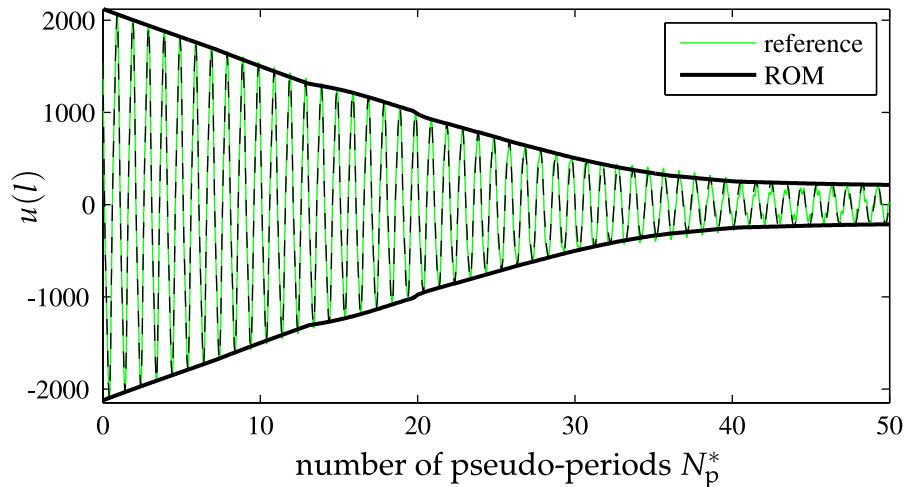


Figure 11: Time history of the free decay from the starting point indicated in Fig. 10c

is depicted for the nonlinear mode based approximation. Details about this approximate synthesis can be found in [1]. The number N_p^* of pseudo-periods was introduced as time variable: It equals $N_p^* = f_0 t$, where f_0 is the eigenfrequency of the considered first mode in the linear case. The results are in reasonably good agreement. Some deviations can be encountered in particular starting from $N_p^* > 35$. This is the time range slightly before and after the friction element is in permanently sticking configuration and the amplitude remains constant. It is conjectured that the non-smooth state transitions between stick and slip are particularly important in this regime and excite other frequencies. This effect cannot be well-resolved with the single nonlinear mode approximation.

Forced response

Finally, the steady-state forced response to harmonic excitation was investigated. A harmonic forcing was applied to the tip of the rod. The forced response was computed by means of the Shooting method applied to the full set of equations of motion in the forced setting.

In Fig. 12, the frequency response curves are depicted for varying excitation level around the first eigenfrequency. The amplitude $u_{\max}(l)$ is defined as the

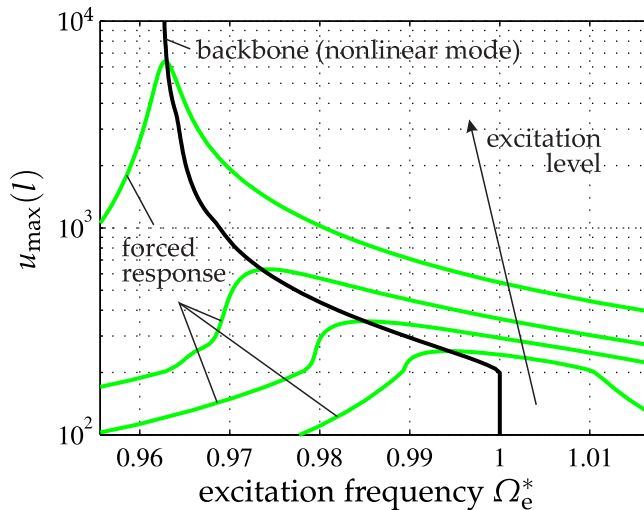


Figure 12: Amplitude-frequency curves of the harmonically forced friction-damped rod and backbone obtained from nonlinear modal analysis

maximum time domain displacement of the rod's tip coordinate $u(\ell)$. The forced response results confirm the softening effect. Moreover, they indicate the decrease of the damping effect, which results in a narrower resonance peak for larger energy levels. The maxima of the frequency response curves also agree quantitatively with the frequency-amplitude characteristic of the nonlinear mode, i. e. the backbone curve.

5. Evaluation of the computational performance

For the two-springs system and the friction-damped rod presented in Section 4.2 and Section 4.3, respectively, the computational effort was investigated. All numerical procedures were implemented and carried out in Matlab R2012a. The simulations were carried out on an Intel Core 2 Quad Q9550 2.83 GHz CPU with 3.62 GB addressable memory. In Table 1 and Table 2, the computational effort for the nonlinear modal analysis is listed.

In the case of the Harmonic Balance (HB) method, the computations were carried out for different harmonic orders H , see e. g. Fig. 7. In general, the number

Table 1: Computational effort for the nonlinear modal analysis (24 data points) of the two-springs system with 2 generalized coordinates

analysis	H	N_t	N_{iter}	computation time in s
HB	1	16	44	0.22
HB	2	16	48	0.25
HB	8	32	47	0.35
HB	20	2048	47	0.90
Shooting	-	128	102	4.2
Shooting	-	256	107	8.4
Shooting	-	1024	104	31.3

N_t of sampling points in the alternating-frequency-time scheme should be selected as large as necessary to ensure sufficient accuracy and as small as possible to avoid spurious computational effort. The optimal number N_t is typically not a priori known and may depend on the harmonic order H . For the smaller harmonic orders $1 \leq H \leq 8$, N_t was selected as the smallest power of two beyond which frequency and damping characteristics did not change significantly anymore. For the largest harmonic order $H = 20$ and $H = 21$, respectively, N_t was set to an unnecessarily large value, just to show its influence on the computation time.

In the case of the Shooting method, the number N_t of time steps in the implicit average acceleration Newmark scheme was varied. Only powers of two were specified. The smallest of the listed numbers was considered just large enough to avoid poor qualitative agreement with the converged results. In order to ensure that the results remain comparable, the same number of data points, i. e. modal amplitudes was considered in the modal analyses. 24 data points were specified in the case of the two-springs system and 80 data points in the case of the friction-damped rod.

For both test cases, sufficiently accurate results can be produced within several seconds. For almost all analyses, the computation time remained below

Table 2: Computational effort for the nonlinear modal analysis (80 data points) of the friction-damped rod with 20 generalized coordinates

analysis	H	N_t	N_{iter}	computation time in s
HB	1	16	152	1.3
HB	3	16	191	2.7
HB	7	32	205	11.2
HB	21	2048	206	99.4
Shooting	-	64	280	9.8
Shooting	-	128	302	11.4
Shooting	-	256	282	20.9
Shooting	-	1024	258	68.3

one minute. In other studies [12, 37] considered similar test cases, but reported computation times of several minutes using a Galerkin-based invariant manifold approach. It is therefore believed that the proposed periodic motion based method is computationally less expensive than invariant manifold based numerical methods. This conclusion seems plausible owing to the typically smaller problem dimension involved in each iteration of the respective approaches, cf. the comment in the introduction.

From a computational point of view, the Harmonic Balance method was considerably less expensive than the Shooting method for the calculations carried out in this study. The benefit of Harmonic Balance appears to be due to both the smaller number of required iterations and the lower computational cost per iteration.

6. Conclusions

A novel definition of the nonlinear modes of nonconservative systems was proposed. They were defined as self-excited limit cycles induced by (typically negative) mass-proportional damping. While the conventional damped motion concept aims at reflecting the strictly autonomous dynamics, the proposed pe-

riodic motion concept is designed to capture the periodic dynamics induced by a resonant excitation source. In a wide range, the numerical examples demonstrated that the extracted modal properties accurately describe the vibration behavior in the vicinity of forced resonances and self-excited limit cycles. This applies to the modal frequency, damping ratio, vibrational deflection shape as well as the asymptotic stability. The limitations of the concept are due to the intrusiveness of the artificial damping term. The concept is fully consistent with the conservative nonlinear or the nonconservative linear case. In the non-conservative nonlinear case, however, the artificial damping term may induce additional modal coupling. Hence, the proposed concept is restricted to the dynamic regimes of isolated nonlinear modes and/or regimes with reasonably low modal damping ratios. Moreover, the definition is limited to periodic motions, and therefore non-periodic regimes which may also occur near resonance, are generally not captured.

An important benefit of the proposed concept is that standard methods for analyzing periodic motions can be applied. Two computational procedures for the modal analysis were described and investigated in this study. One of them is based on the Harmonic Balance method and one on the Shooting method. It is noteworthy that the Harmonic Balance based procedure degenerates to the well-known harmonic linearization technique if the model comprises only a single degree of freedom. Both procedures are applicable to generic nonlinearities, including those involving non-smooth forces. Their computational performance is comparatively good, even if the model features a larger number of generalized coordinates.

The overall approach is regarded as an effective and computationally efficient tool for modal parameter extraction of nonconservative nonlinear systems in the aforementioned dynamic regimes. Since the energy-dependent modal properties accurately reflect the resonant vibration behavior, they represent relevant measures for the structural dynamic design of nonlinear structures. For instance, the proposed approach gives directly rise to a measure of the damping effectiveness. This is obviously a crucial feature for the design assessment of vibration

reduction mechanisms such as friction damping. As it was demonstrated in previous works [17, 1], the modal characteristics can also be utilized for model reduction. This facilitates quantitatively accurate vibration predictions for a wide range of operating conditions.

References

- [1] M. Krack, L. Panning-von Scheidt, J. Wallaschek, On the computation of the slow dynamics of nonlinear modes of mechanical systems, *Mechanical Systems and Signal Processing* 42 (1-2) (2014) 71–87.
- [2] M. Krack, S. Tatzko, L. Panning-von Scheidt, J. Wallaschek, Reliability Optimization of Friction-Damped Systems Using Nonlinear Modes, *Journal of Sound and Vibration* 333 (2014) 2699–2712.
- [3] G. Kerschen, M. Peeters, J. C. Golinval, A. F. Vakakis, Nonlinear Normal Modes, Part I: A Useful Framework for the Structural Dynamicist: Special Issue: Non-linear Structural Dynamics, *Mechanical Systems and Signal Processing* 23 (1) (2009) 170–194.
- [4] A. Vakakis, L. Manevitch, Y. Mikhlin, V. Pilipchuk, A. Zevin, *Normal Modes and Localization in Nonlinear Systems*, John Wiley & Sons, New York, 2008.
- [5] R. M. Rosenberg, Normal Modes of Nonlinear Dual-Mode Systems, *Journal of Applied Mechanics* 27 (1960) 263–268.
- [6] R. H. Rand, A Direct Method for Non-Linear Normal Modes, *International Journal of Non-Linear Mechanics* 9 (5) (1974) 363–368.
- [7] D. Laxalde, F. Thouverez, Complex Non-Linear Modal Analysis for Mechanical Systems Application to Turbomachinery Bladings With Friction Interfaces, *Journal of Sound and Vibration* 322 (4-5) (2009) 1009–1025.
- [8] S. W. Shaw, C. Pierre, Non-Linear Normal Modes and Invariant Manifolds, *Journal of Sound and Vibration* 150 (1) (1991) 170–173.

- [9] S. W. Shaw, C. Pierre, Normal Modes for Non-Linear Vibratory Systems, *Journal of Sound and Vibration* 164 (1) (1993) 85–124.
- [10] S. W. Shaw, C. Pierre, Normal Modes of Vibration for Non-Linear Continuous Systems, *Journal of Sound and Vibration* 169 (3) (1994) 319–347.
- [11] F. Blanc, C. Touzé, J.-F. Mercier, K. Ege, A.-S. Bonnet Ben-Dhia, On the Numerical Computation of Nonlinear Normal Modes for Reduced-Order Modelling of Conservative Vibratory Systems, *Mechanical Systems and Signal Processing* 36 (2) (2013) 520–539.
- [12] L. Renson, G. Deliége, G. Kerschen, An Effective Finite-Element-Based Method for the Computation of Nonlinear Normal Modes of Nonconservative Systems, *Meccanica* (2014) 1–16.
- [13] W. Szemplinska-Stupnicka, The Modified Single Mode Method in the Investigations of the Resonant Vibrations of Non-Linear Systems, *Journal of Sound and Vibration* 63 (4) (1979) 475–489.
- [14] J. Náprstek, Non-linear auto-parametric vibrations in civil engineering systems, in: B. H. V. Topping, L. C. Neves, R. C. Barros (Eds.), *Trends in Civil and Structural Engineering Computing*, Saxe-Coburg Publications, 2009, pp. 293–317.
- [15] A. Tondl, *Autoparametric resonance in mechanical systems*, Cambridge University Press, 2000.
- [16] M. Peeters, G. Kerschen, J. C. Golinval, Dynamic Testing of Nonlinear Vibrating Structures Using Nonlinear Normal Modes, *Journal of Sound and Vibration* 330 (3) (2011) 486–509.
- [17] M. Krack, L. Panning-von Scheidt, J. Wallaschek, A Method for Nonlinear Modal Analysis and Synthesis: Application to Harmonically Forced and Self-Excited Mechanical Systems, *Journal of Sound and Vibration* 332 (25) (2013) 6798–6814.

- [18] T. M. Cameron, J. H. Griffin, An Alternating Frequency/Time Domain Method for Calculating the Steady-State Response of Nonlinear Dynamic Systems, *Journal of Applied Mechanics* 56 (1) (1989) 149–154.
- [19] A. Cardona, T. Coune, A. Lerusse, M. Geradin, A Multiharmonic Method for Non-Linear Vibration Analysis, *International Journal for Numerical Methods in Engineering* 37 (9) (1994) 1593–1608.
- [20] M. Berthillier, C. Dupont, R. Mondal, J. J. Barrau, Blades Forced Response Analysis with Friction Dampers, *Journal of Vibration and Acoustics* 120 (2) (1998) 468–474.
- [21] C. Siewert, L. Panning, J. Wallaschek, C. Richter, Multiharmonic Forced Response Analysis of a Turbine Blading Coupled by Nonlinear Contact Forces, *Journal of Engineering for Gas Turbines and Power* 132 (8) (2010) 082501/1–082501/9.
- [22] R. Seydel, *Practical Bifurcation and Atability Analysis: from Equilibrium to Chaos*, Springer New York, 1994.
- [23] G. v. Groll, D. J. Ewins, The Harmonic Balance Method With Arc-Length Continuation in Rotor/Stator Contact Problems, *Journal of Sound and Vibration* 241 (2) (2001) 223–233.
- [24] A. Lazarus, O. Thomas, A harmonic-based method for computing the stability of periodic solutions of dynamical systems, *Comptes Rendus Mécanique* 338 (9) (2010) 510–517.
- [25] M. Peeters, R. Vignié, G. Sérandour, G. Kerschen, J. C. Golinval, Nonlinear normal modes, Part II: Toward a practical computation using numerical continuation techniques: Special Issue: Non-linear Structural Dynamics, *Mechanical Systems and Signal Processing* 23 (1) (2009) 195–216.
- [26] K. Magnus, K. Popp, *Schwingungen*, Teubner, Stuttgart, 1997.

- [27] S. Bellizzi, R. Bouc, A New Formulation for the Existence and Calculation of Nonlinear Normal Modes, *Journal of Sound and Vibration* 287 (3) (2005) 545–569.
- [28] C. Touzé, M. Amabili, Nonlinear Normal Modes for Damped Geometrically Nonlinear Systems: Application to Reduced-Order Modelling of Harmonically Forced Structures, *Journal of Sound and Vibration* 298 (4–5) (2006) 958–981.
- [29] A. A. Ferri, Friction Damping and Isolation Systems, *Journal of Vibration and Acoustics and Journal of Mechanical Design / 50th Anniversary of the ASME Design Engineering Division* 117 (B) (1995) 196–206.
- [30] K. Popp, L. Panning, W. Sextro, Vibration Damping by Friction Forces: Theory and Applications, *Journal of Vibration and Control* 9 (3-4) (2003) 419–448.
- [31] R. Elliott, S. Patsias, P. Doody, Optimisation of Turbine Blade Shroud and Under-Platform Dampers: Part 2 - Numerical Predictions, *Proceedings of the 12th International Symposium on Transport Phenomena and Dynamics of Rotating Machinery*, February 17-22, Honolulu, HI, USA, pp. 1–9 (2008).
- [32] A. Sinha, J. H. Griffin, Friction Damping of Flutter in Gas Turbine Engine Airfoils, *AIAA Journal of Aircraft* 20 (4) (1983) 372–376.
- [33] W. E. Whiteman, A. A. Ferri, Suppression of Bending-Torsion Flutter through Displacement-Dependent Dry Friction Damping, *AIAA Journal* 37 (1) (1999) 79–83.
- [34] R. D. Cook, *Concepts and Applications of Finite Element Analysis*, 4th Edition, John Wiley & Sons, New York, 2002.
- [35] W. E. Whiteman, A. A. Ferri, Displacement-Dependent Dry Friction Damping of a Beam-Like Structure, *Journal of Sound and Vibration* 198 (3) (1996) 313–329.

- [36] Y. P. Zaspá, Nonlinear Shapes of Steady-State Vibrational Oscillations of Mechanical Contact. Symmetrical Tangential Oscillations, *Journal of Friction and Wear* 28 (1) (2007) 87–104.
- [37] L. Renson, Nonlinear Modal Analysis of Conservative and Nonconservative Aerospace Structures, Ph.D. thesis, Université de Liège, Liège (2014).